Conf-820745--1

BNL 31674

BNL--31674

DE82 020376

STRANGENESS EXCHANGE REACTIONS AND HYPERNUCLEI

Carl B. Dover
Brookhaven National Laboratory
Upton, New York 11973

BNL 31674

STRANGENESS EXCHANGE REACTIONS AND HYPERNUCLEI

by

Carl B. Dover
Brookhaven National Laboratory
Upton, New York 11973

ABSTRACT

Recent progress in the spectroscopy of Λ and Σ hypernuclei is reviewed. Prospects for the production of doubly strange hypernuclei at a future kaon factory are assessed. It is suggested that the (K^-,K^+) reaction on a nuclear target may afford an optimal way of producing the H dibaryon, a stable six quark object with $J^\pi=0^+, S=-2$.

I. INTRODUCTION

The purpose of this talk is two-fold: firstly, I would like to briefly review the progress of the last few years on the spectroscopy of Λ and Σ hypernuclei (strangeness $S=-1$), as seen in the strangeness exchange (K^-,π) reaction on nuclear targets. New theoretical insights into hypernuclear structure have emerged from significant experimental advances at Brookhaven and CERN. Several of the open questions will be explored, particularly those involving the widths and coupling schemes for Σ hypernuclei. As an example of the sort of experiments which could greatly benefit from intense beams at a future kaon factory, we discuss the double strangeness exchange (K^-,K^+) reaction, leading to Ξ or $\Lambda\Lambda$ hypernuclear systems. The (K^-,K^+) reaction on a ^{3}He target is proposed as a very promising way of looking for the H particle, an $S=-2$ six quark dibaryon predicted by the MIT Bag Model.

II. PROGRESS IN Λ HYPERNUCLEAR SPECTROSCOPY

Recently, there have been a number of reviews of hypernuclear physics[1-6]. Rather than attempting a complete exposé here, we refer the reader to the literature[1-6], particularly the extensive review of Dover and Walker[5].

The basic single strangeness exchange reactions which have been used to produce Λ and Σ hypernuclei are $K^-n\to\pi^-\Lambda$, $K^-n\to\pi^-\Sigma^0$, $K^-p\to\pi^-\Sigma^+$ and $K^-p\to\pi^+\Sigma^-$. In Figs. 1 and 2, we display the momentum dependence of the 0° differential cross sections for $K^-n\to\pi^-\Lambda$ and $K^-p\to\pi^+\Sigma^-$ reactions. The dashed lines show the free space two-body cross sections, while the solid lines represent two types of Fermi average[5], either of the cross section $\langle d\sigma/d\Omega_L\rangle_{AV}$ or the amplitude $\langle f_L\rangle_{AV}$. The effect of averaging is to modulate the rapid energy dependences seen in the free cross sections, as expected. The (K^-,π) cross sections for both Λ and Σ production are seen to be of quite reasonable size, i.e., one or a few mb/sr at 0°. This has enabled one to produce measurable numbers of hypernuclei, using even the rather feeble kaon intensities in existing beams.

The well-known momentum transfer characteristics of the (K^-,π) reaction are shown in Fig. 3. At a "magic momentum" of about 280 MeV/c for Σ production and 330 MeV/c for Λ production, the forward momentum transfer $q(0^\circ)$ vanishes, resulting in a Σ or Λ at rest in the nucleus. Thus, the (K^-,π) reaction in this momentum range emphasizes the production of low spin substitutional states, in which a nucleon in a given shell model orbit $\{\ell,j\}$ is simply replaced by a Λ or Σ in the same orbit. Higher spin states emerge at non-zero angles (for p-shell spin-zero nuclear targets, 0^+ hypernuclear states peak at 0° in the (K^-,π) reactions, 1^- at about 10°, etc.). The shape of the (K^-,π) angular distribution provides a clear signature for the spin of an isolated hypernuclear state (as in other nuclear reactions). In Fig. 3, we also show $q(0^\circ)$ as a function of lab momentum for the associated production processes $\pi N\to K\Lambda, K\Sigma$. Here, the momentum transfer remains larger than the nuclear Fermi momentum in the region 1.1-1.5 GeV/c where the two-body cross section is largest. Thus, the (π,K^+) reaction is expected to populate high spin Λ and Σ hypernuclear states, and serve as a useful complement to the $(\bar{K},\pi)$ reaction studies. The reader is referred to ref. 7 for a detailed theoretical discussion of the expected cross sections for the (π,K) reaction on nuclear targets; no experimental data yet exists.

The first (K^-,π^-) survey experiments involving a range of nuclear targets were performed by the CERN group[8,9]. A global view of their results[10] is given in Fig. 4. The excitation functions shown are all for 0° (pion angle) and a K^-

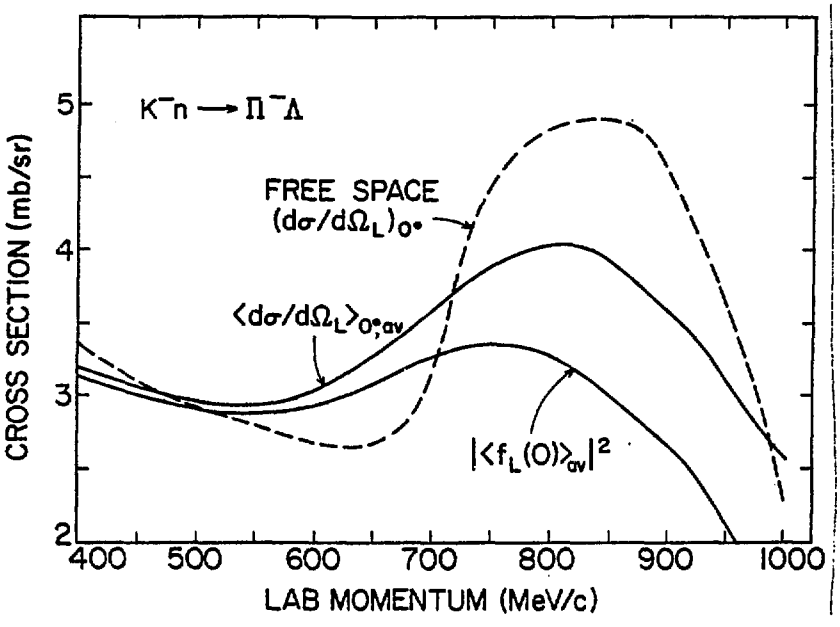

Fig. 1.
Fermi-averaged cross sections at 0° for $K^-n \rightarrow \pi^-\Lambda$.

Fig. 2.
Fermi-averaged 0° cross sections for $K^-p \rightarrow \pi^+\Sigma^-$.

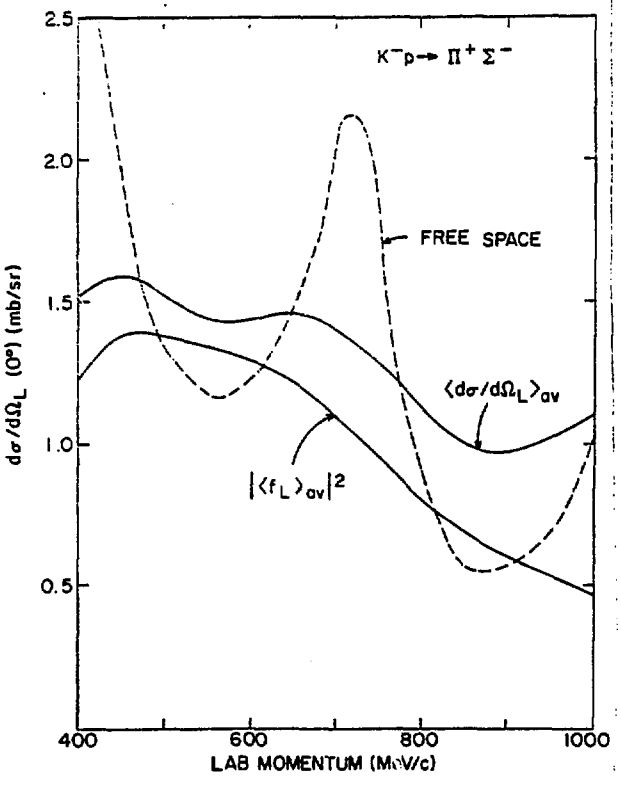

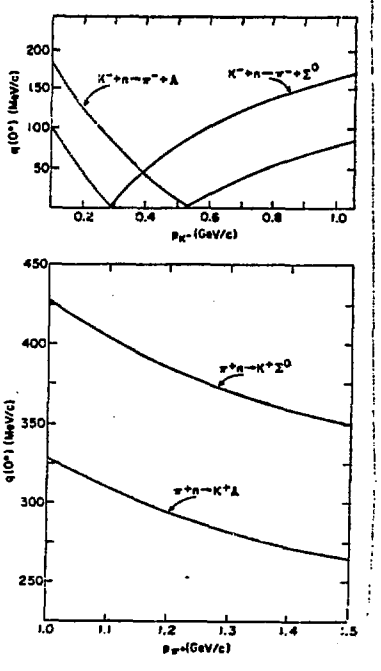

Fig. 3.
Forward momentum transfer as a function of lab momentum.

momentum in the range 700-800 MeV/c. The energy resolution is rather coarse (3-5 MeV), so one is unable to resolve any fine structure in the hypernuclear spectrum (these spectra are perhaps reminiscent of an early stage of nuclear structure physics, before high resolution spectrometers became available). In the simplest theoretical picture, the peaks seen in Fig. 4 are interpretable in terms of dominant Λ particle-neutron hole excitations, mostly of substitutional character $(\ell j)_n \rightarrow (\ell j)_\Lambda$. A more detailed view of the CERN (K^-,π^-) spectra[9] for the light targets ^{6}Li through ^{12}C is shown in Fig. 5. The shaded areas indicate the part of cross section attributable to the transition $(S_{1/2})_n \rightarrow (S_{1/2})_\Lambda$. This identification is rather clear in $^6_\Lambda$Li and $^7_\Lambda$Li, but becomes more problematical in the heavier systems $^9_\Lambda$Be and $^{12}_\Lambda$C, due to the sizable spreading width of the $S_{1/2}$ neutron hole state.

The 0° spectra of Figs. 4 and 5, because of the coarse energy resolution, do not yield any serious constraints on the spin dependence of the Λ-nucleon residual interaction. More recently, angular distributions for the (K^-,π^-) reaction have been measured[11,12] at the Brookhaven AGS. Because of the strong variation of q with pion angle, states of different spin are preferentially excited as the angle is varied. Some of the experimental results[12] are shown in the top half of Fig. 6. At different angles, the relative intensities of the peaks change, and there are also energy shifts which are directly related to the properties of the Λ-N interaction.

A detailed analysis of the $^{13}_\Lambda$C data, leading to an understanding of the (K^-,π^-) reaction mechanism as well as the extraction of constraints on the Λ-N interaction, has been given in refs. 13 and 14. For analyses of this type, a comprehensive shell model code for light Λ and Σ hypernuclei has been developed at Brookhaven[13,14], and applied throughout the P-shell. The calculations employ the distorted wave impulse approximation (DWIA), with K^- and π^- distorted waves generated by a Woods-Saxon potential, the parameters of which are adjusted to fit the K^- and π^- elastic scattering data[15] on the neighboring nucleus ^{12}C at 800 MeV/c. The quality of these fits is shown in Fig. 7, taken from ref. 14. The "tδ" approximation to either the K^- or π^- optical potential (even using a Fermi averaged $\bar{K}N$ or πN amplitude t) does not yield a quantitative description of the elastic data; a good fit to the elastic data turns out to be important in obtaining the correct (K^-,π^-) absolute cross sections. The Fermi-averaged $K^-n \rightarrow \pi^-\Lambda$ amplitude $\langle f_L(0)\rangle_{AV}$ of Fig. 1 is used to obtain a transition matrix element. Neutron and Λ bound state wave functions were generated[14] from Woods-Saxon

potentials adjusted to fit single particle energies and electron scattering information.

The differential (K^-,π^-) cross section to a particular Λ hypernuclear state involves the amplitudes $M^{(\Delta L)}(\theta)$, arising from the DWIA integration over distorted waves. For the non-spin-flip processes which dominate the (K^-,π^-) reaction, ΔL = orbital angular momentum transfer = ΔJ; for a single particle transition $\ell_N \rightarrow \ell_\Lambda$, with a closed shell target, one has the natural parity selection rule $\Delta L + \ell_N + \ell_\Lambda$ = even. The amplitudes $M^{(\Delta L)}(\theta)$ peak at different characteristic values of θ for different ΔL. Starting from the $\frac{1}{2}^-$ target ^{13}C, $M^{(0)}$ leads to the excitation of $\frac{1}{2}^-$ states in $^{13}_{\Lambda}C$ via $p_N \rightarrow p_\Lambda$ transitions and peaks at 0°. For an incident momentum of 800 MeV/c, the $p_N \rightarrow S_\Lambda$ transition amplitude $M^{(1)}$ peaks at about 10°. Near 15°, the amplitude $M^{(2)}$ has its peak, and here it dominates the contribution of $M^{(0)}$ to $p_N \rightarrow p_\Lambda$ transitions; note that $M^{(2)}$ leads to $3/2^-$ and $5/2^-$ states in $^{13}_{\Lambda}C$, rather than $\frac{1}{2}^-$ for $M^{(0)}$. The measurement of the energy shifts of peaks between 0° and 15° then yields some idea of the size of the Λ-N residual interaction.

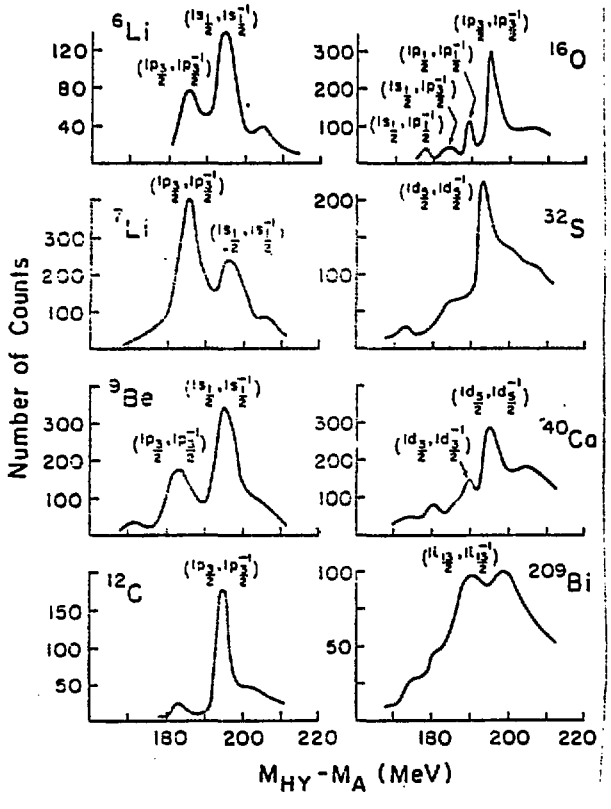

Fig. 4.
Forward cross sections for the (K^-,π^-) reaction on various nuclear targets.

The theoretical (K^-,π^-) spectra for a ^{13}C target are shown in the bottom half of Fig. 6, binned as in the experiment for easier comparison. The contribution of each ΔL is shown separately, and displays the characteristic angular dependence just discussed. In Fig. 8, the full angular distributions for three of the peaks are shown. The DWIA is seen to agree well with the data, both in absolute cross sections and angular shapes; this gives us some confidence in the spin assignments deduced from the data.

Some of the main features of the spectroscopy of $^{13}_{\Lambda}C$ emerge from a weak coupling picture, but in some cases there are striking changes due to the Λ-N residual interaction. Core excitations in ^{12}C play an important role; in addition to the $0^+(T=0)$ ground state, strong excitations in $^{13}_{\Lambda}C$ are seen involving a Λ coupled to the $2^+(T=0)$, $1^+(T=0)$, $1^+(T=1)$ and $2^+(T=1)$ excited states of ^{12}C at 4.4, 12.7, 15.1 and 16.1 MeV, respectively. In the weak coupling picture, the (K^-,π^-) strength associated with a certain core state is proportional to the neutron pickup strength, known for instance from the $^{13}C(p,d)^{12}C^*$ reaction. The pattern of pickup strength[14] is shown in Fig. 9; a poor resolution experiment, which sums over groups of final states, sees just this strength. In the weak coupling picture, based on Fig. 9 one can easily seen that five peaks with measurable cross section are expected in the $^{13}_{\Lambda}C$ spectrum. This is the main qualitative feature of the experimental spectrum shown in Fig. 6.

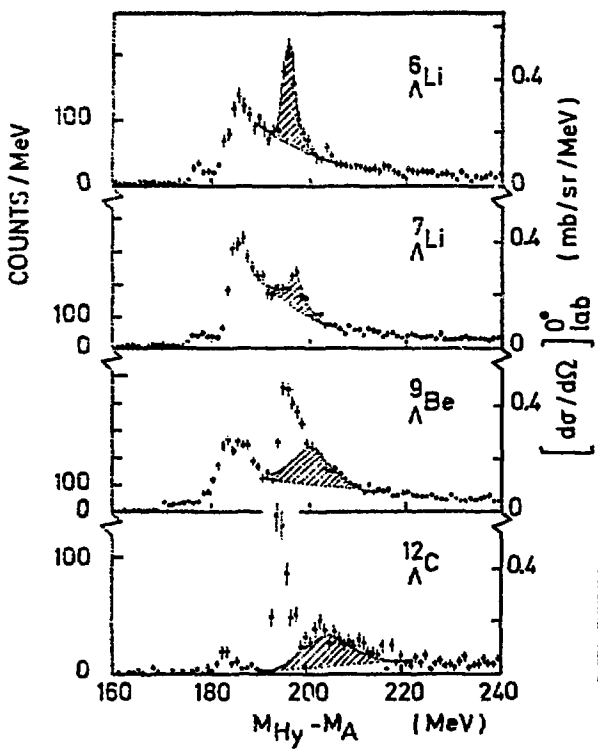

Fig. 5.
(K^-,π^-) cross sections at 0°; the shaded area represents the $S_N \rightarrow S_\Lambda$ transition strength

The more interesting physics of $^{13}_{\Lambda}C$ is revealed in the departure of energies and relative intensities from the weak coupling picture. These differences are generated by the Λ-N residual interaction. The analysis is discussed in detail in refs. 13 and 14; we present only the main results here. We consider an interaction of the form

$$V_{\Lambda N}(r) = V_o(r)(1-\varepsilon+\varepsilon P_x)(1+\alpha \underset{\sim}{\sigma}_N \cdot \underset{\sim}{\sigma}_\Lambda) + V_\pm(r)(\underset{\sim}{\sigma}_\Lambda \pm \underset{\sim}{\sigma}_N)\cdot \underset{\sim}{\ell}_{N\Lambda}, \quad (1)$$

the usual Slater integrals $F^{(k)}$ are given in terms of a multiple expansion:

$$V_o(\underset{\sim}{r}_N - \underset{\sim}{r}_\Lambda) = \sum_{k=0}^{\infty} V_k(r_N, r_\Lambda) P_k(\cos\theta_{\underset{\sim}{r}_N, \underset{\sim}{r}_\Lambda})$$

$$F^{(k)} = \int R^2_{\ell_N}(r_N) R^2_{\ell_\Lambda}(r_\Lambda) V_k(r_N, r_\Lambda) dr_N dr_\Lambda \quad . \tag{2}$$

For $\ell_N = \ell_\Lambda = 1$, only $F^{(0)}$ and $F^{(2)}$ enter. We assumed[14] $F^{(0)} = -1.6$, $\alpha = -0.1$, $\epsilon = 0$ and used the energy differences and relative intensities of the observed peaks in $^{13}_{\Lambda}C$ to constrain $F^{(2)}$ and the Λ spin-orbit splitting ε_p; the latter receives contributions from the symmetric and antisymmetric two-body spin-orbit potentials of Eq. (1) and also from a one-body spin-orbit term we have added.

Our conclusions are as follows: i) from a 0.36±0.3 MeV shift[12] in the energy of the "10 MeV" peak as we pass from 0° to 15°, we obtain a small Λ spin-orbit splitting $\varepsilon_p \approx 0.5$ MeV, consistent with the earlier conclusion of the CERN group[8,16]; ii) from a 1.7±0.4 MeV shift of the "16 MeV" peak between 0° and 15°, we obtain limits $-3.4 < F^{(2)} < -3.1$ MeV for the strength of the ΛN quadrupole-quadrupole potential. Thus, even from a coarse resolution experiment, we can obtain non-trivial constraints on $V_{\Lambda N}(r)$. High resolution (K^-,π^-) data on a variety of p-shell targets are required before one can sort out the details of the spin-spin and spin-orbit parts of the two-body force. Very recent data[17] obtained at Brookhaven on the $(K^-,\pi^-\gamma)$ reaction give accurate values (to 100 keV or so) for the energy difference between certain hypernuclear levels. For example, in $^{7}_{\Lambda}Li$, a hypernuclear γ ray with an energy of 2 MeV is seen[17], close to the energy difference of 2.18 MeV for the relevant core states in

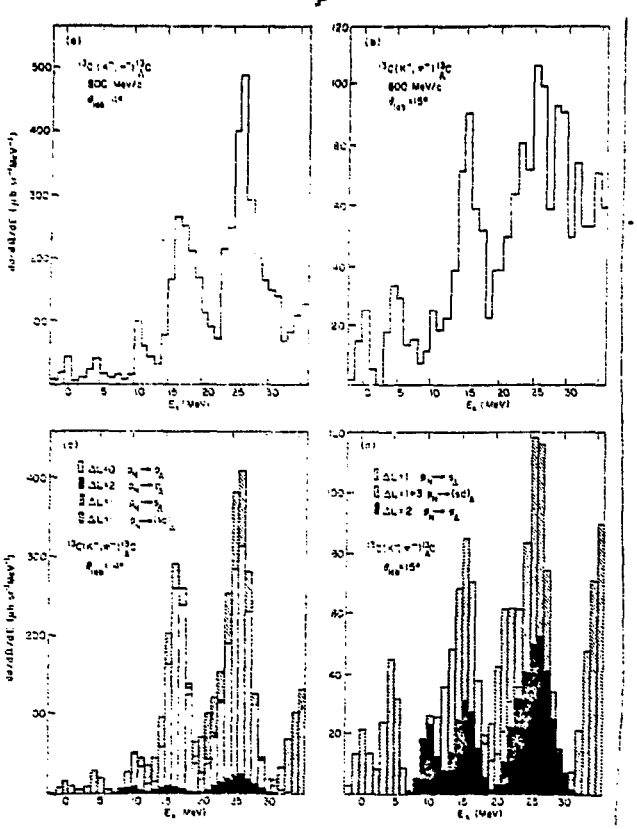

Fig. 6.
Experimental and theoretical cross sections for $^{13}C(K^-,\pi^-)^{13}_{\Lambda}C$ at 800 MeV/c.

^{6}Li. This indicates that the spin dependence of the ΛN potential is weaker than anticipated in ref. 18, although a detailed analysis remains to be done.

The most interesting aspects of the $^{13}_{\Lambda}$C spectrum are the energy splitting ΔE and intensity ratio R of the 16 and 10 MeV peaks at 0°. Here, the weak coupling basis states $|0^+(T=0)\theta_\Lambda P_{1/2}>_{1/2^-}$ and $|2^+(T=0)\theta_\Lambda P_{3/2}>_{1/2^-}$ are significantly mixed by $F^{(2)}$. If we write

$$|1/2^-\rangle_1 = \alpha|0^+\theta_\Lambda P_{1/2}\rangle - \beta|2^+\theta_\Lambda P_{3/2}\rangle \qquad (3)$$

then

$$R = (\beta\theta(1/2)+\alpha\theta(3/2))^2/(\alpha\theta(1/2)-\beta\theta(3/2))^2,$$

where θ(1/2) and θ(3/2) are the spectroscopic amplitudes for neutron pickup from the ^{13}C ground state to the first 0^+ and 2^+ states of ^{12}C, respectively. With no mixing, and using Cohen-Kurath wave functions[19], one obtains R=1.8. The experimental value[12] is R ≈ 5, while the theoretical values

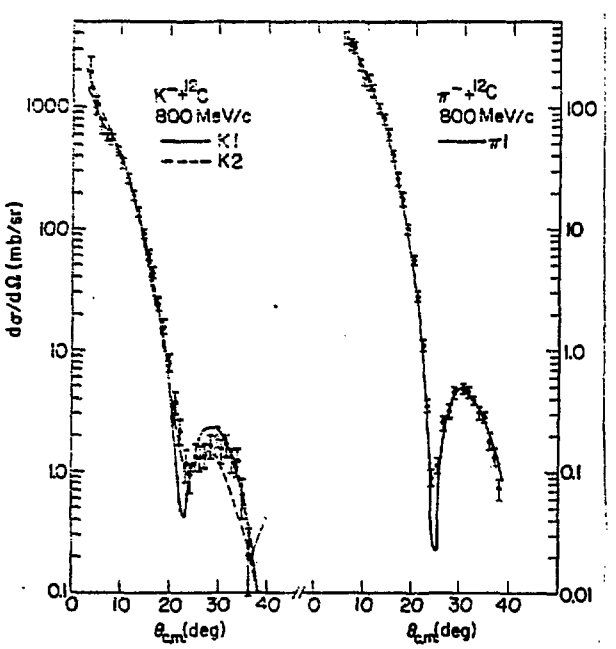

Fig. 7.

Optical model fits to K^- and π^- elastic scattering data on ^{12}C.

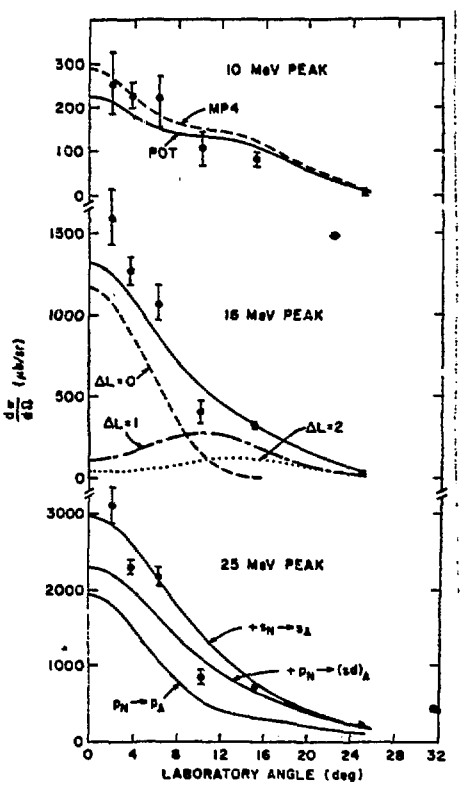

Fig. 8.

Angular distributions for the $^{13}C(K^-,\pi^-)^{13}_{\Lambda}C$ reaction to various final states.

one obtains with mixing ($\alpha \approx 0.96, \beta \approx 0.28$, $F_2 \approx -3$ to -3.5 MeV) are $R \approx 6$-7. If one makes ε too large, R increases to unacceptably large values.

Despite the relatively weak ΛN force, the hypernucleus displays a tendency to seek a higher degree of spatial symmetry in the lowest $1/2^-$ state. If instead of the weak coupling basis, we used the states of [54] and [441] symmetry, the first $1/2^-$ is dominantly the [54] symmetry, which is forbidden by the Pauli principle for a system of nucleons. In the limit where [54] symmetry is exact for this $1/2^-$ state, one has a dynamical selection rule inhibiting its population in the (K^-,π^-) reaction, since a [54] symmetry is unreachable with $\Delta L=0$, starting with the dominant [441] of the ^{13}C ground state. This tendency towards spatial symmetry (increased by using $\varepsilon>0$) accounts for the strong deviation of R from its pick-up value in the weak coupling limit.

The full exploitation of the structure information available from Λ-hypernuclear spectra clearly requires a considerable improvement in energy resolution, available only with more intense K^- beams.

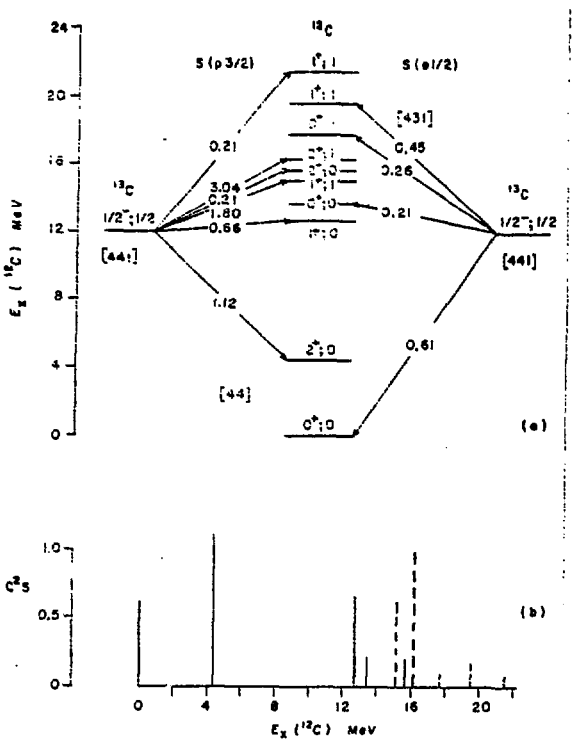

Fig. 9.

Neutron pickup strength from ^{13}C to various states in ^{12}C.

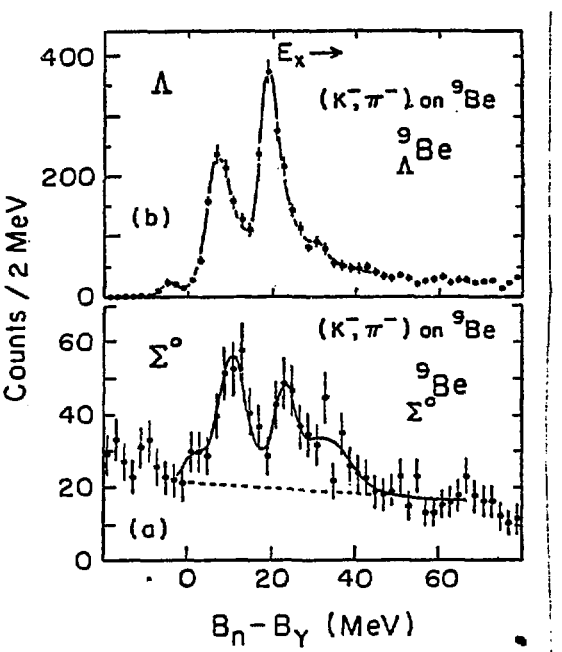

Fig. 10.

Cross sections at 0° for production of $^9_\Lambda Be$ and $^9_\Sigma Be$ in the (K^-,π^-) reaction.

III. PROGRESS IN Σ HYPERNUCLEAR SPECTROSCOPY

The first evidence for relatively narrow Σ states in nuclei was reported by the CERN group[20]. They studied the forward production of Σ's in the $(K^-,\pi^\pm)$ reaction at 720 MeV/c. Targets of ^{6}Li, ^{7}Li, ^{9}Be, and ^{12}C were used. The clearest evidence for narrow Σ structures was seen in the $^9\text{Be}(K^-,\pi^-)^9_\Sigma\text{Be}$ data, reproduced in Fig. 10. The data for the same process in the Λ region are also shown. More recently, the reaction $^6\text{Li}(K^-,\pi^+)^6_\Sigma\text{H}$ at 713 MeV/c was studied[21] at the Brookhaven AGS. The 4° spectrum in the Σ region is shown in Fig. 11. There is clear evidence for two peaks superimposed on a quasielastic background. At the Heidelberg meeting[6], the CERN group[22] reported preliminary data on the reactions $^{12}\text{C}(K^-,\pi^\pm)$ and $^{16}\text{O}(K^-,\pi^+)$ at 450 MeV/c, and $^{12}\text{C},^{16}\text{O}(K^-,\pi^-)$ at 400 MeV/c. These experiments were run in a redesigned beam line at CERN, specifically set up for running at very low momentum, near the "magic momentum" of Fig. 3. Narrow Σ states were seen at both 400 and 450 MeV/c, in both the (K^-,π^-) and (K^-,π^+) channels. Presumably, these correspond to the coherent substitutional transitions $p_N \rightarrow p_\Lambda$ with $\Delta L=0$, leading to 0^+ final states.

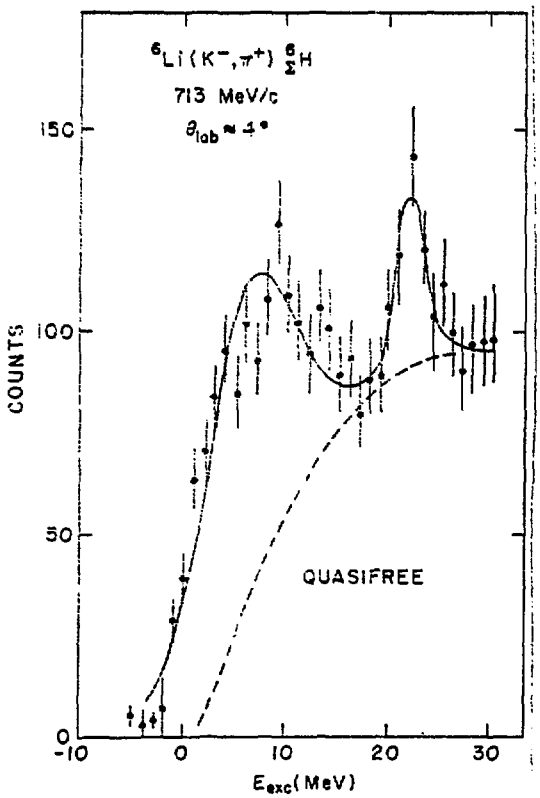

Fig. 11.
Forward angle cross section for the reaction $^6\text{Li}(K^-,\pi^+)^6_\Sigma\text{H}$.

In the interpretation of Σ hypernuclear spectra, a number of interesting questions arise, which include the following: What are the single particle properties of a Σ in the nucleus, i.e. the well depths of the central and spin-orbit potentials? Do the Σ states have a good isospin? Why are some Σ states relatively narrow? The data are as yet too crude to permit definitive answers to these questions, but some progress has been made. For instance, the data on Σ^--atoms already suggested[23] a well depth for the Σ of order 26 MeV, somewhat shallower than for the Λ. The $(K^-,\pi^\pm)$ data are consistent with this, if one compares the

excitation energy of Λ and Σ peaks corresponding to the same $p_N \rightarrow p_{\Lambda,\Sigma}$ transition. The Σ spin-orbit potential is more controversial. Meson exchange models[24] predict a fairly small spin-orbit splitting for the Σ, while naive quark model considerations[25] yield a splitting comparable to that for the nucleon. The simplest interpretation of the preliminary CERN data[22] would suggest a sizable Σ spin-orbit potential. However, this ignores the effect of the ΣN residual interaction. The free space ΣN potentials for Models D and F of deSwart and collaborators[26] are shown in Fig. 12. Unlike the ΛN case, the ΣN potential exhibits a strong spin and isospin dependence; it is not known how this dependence is altered as we pass to an effective interaction in the nuclear medium. If we calculate the Σ particle-nucleon hole matrix elements of the free $V_{\Sigma N}$, we find that in some case coherent shifts[27] of Σ-hypernuclear states occur. For instance, in $^{12}_{\Sigma}C$ and $^{16}_{\Sigma}O$, 0^+(I=3/2) states are shifted upward while 0^+(I=1/2) states are shifted downward. The questions of isospin purity and coupling schemes (jj, LS, etc.) for Σ states are open at this point. There could be interesting deviations from the weak coupling limit. However, it will be difficult to develop a phenomenology of ΣN interactions unless a number of narrow Σ states are seen. The experiments to date are intriguing, but more data (of higher quality) are required. The CERN data is restricted to forward angles, so substitutional 0^+ states are emphasized. A very important question is whether higher spin Σ states are also narrow in some cases; so far there is no evidence for the production of a narrow hypernuclear ground state. Angular distributions for the $(K^-,\pi^\pm)$ reactions are necessary in order to settle this question and to obtain definite spin assignments. An intense low momentum K^- beam at a kaon factory would be of enormous benefit in the study of Σ hypernuclei.

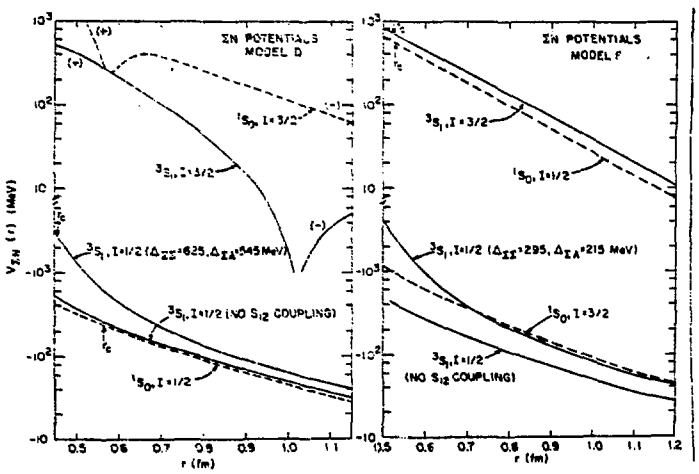

Fig. 12.
Free space ΣN potentials for I=0.

The widths of Σ hypernuclear states have been discussed by several authors[28,29]. Many of these papers[29] are concerned with various nuclear medium corrections (Pauli, dispersion

and binding effects, for instance) to the naive optical model estimate $\Gamma \approx 2W(0) \approx 30$ MeV obtained for a very deeply bound Σ state from the depth $W(0)$ of the absorptive part of the Σ^--atom potential[23]. These corrections tend to decrease the Σ width due to $\Sigma N \to \Lambda N$ conversion significantly. Of the calculations listed in ref. 29, those due to Johnstone and Thomas are most relevant, since they pertain to specific Σ orbitals in finite nuclei. They predict that even the Σ ground states may be narrow enough to be observable for some light systems.

The optical model picture, even after the inclusion of medium corrections, neglects an important feature of $\Sigma N \to \Lambda N$ conversion, namely its spin-isospin selectivity[28]. At low momentum the dominant contribution to conversion arises from the $^3S_1$, I=1/2 partial wave. Dynamically, this arises because of the ΣN initial state interactions, which are strongly attractive for $^3S_1$, I=1/2 and repulsive for $^1S_0$, I=1/2. The attraction focuses the wave function so that conversion takes place more easily. In addition, the tensor part of π and ρ exchange is kinematically favored in the 80 MeV $\Sigma N \to \Lambda N$ conversion.

In heavy nuclei, where spins and isospins are close to saturation, this selectivity has little consequence. For light systems, its effects are more pronounced. In its simplest form, the expectation value of the transition operator $\Sigma_i \delta(\underset{\sim}{r}_i - \underset{\sim}{r}_\Sigma)$ which occurs in the optical model must be replaced by $1/12 \Sigma_i \delta(\underset{\sim}{r}_i - \underset{\sim}{r}_\Sigma)(3+\underset{\sim}{\sigma}_i \cdot \underset{\sim}{\sigma}_\Sigma)(1-\underset{\sim}{\tau}_i \cdot \underset{\sim}{t}_\Sigma)$. This operator is to be sandwiched between hypernuclear wave functions which depend explicitly on spin and isospin. Depending on the total spin J and isospin I of the Σ hypernuclear levels, as well as the details of the coupling scheme, one obtains widths which are sometimes quenched and sometimes increased with respect to the optical model limit.

The most dramatic effects of selectivity are found for 0^+ states of maximum isospin formed by the coherent replacement $(\ell j)_N \to (\ell j)_\Sigma$. For example, in a simple j-j coupling picture of $^{12}_{\Sigma}C$, the width of the coherent $(_N P^{-1}_{3/2} \; _\Sigma P_{3/2})_{0^+,I}$ states changes significantly from the nuclear matter value $\Gamma = \Gamma_s + \Gamma_p$ to $\Gamma(0^+, I=1/2) = \Gamma_s + 12/7 \Gamma_p$ and $\Gamma(0^+, I=3/2) = \Gamma_s$. For the I=3/2 state, the Σ^- annihilation on P-shell nucleons is totally suppressed by the presence of spin-isospin correlations in the initial j-j hypernuclear wave function. The quenching factor $\Gamma_s / \Gamma_s + \Gamma_p$ assumes the value 0.41 if one uses oscillator wave functions, so a total width of the order of 5 MeV might be anticipated for the 0^+, I=3/2 excitation in $^{12}_{\Sigma}Be$. The predicted widths depend on the degree of isospin purity of the Σ states. Clearly, the isospin selectivity of the $\Sigma N \to \Lambda N$

conversion process loses much of its punch if one has appreciable isospin mixing in Σ hypernuclear states. The ratio of the widths of 0^+ states ($p_N \to p_\Sigma$) in ${}^{12}_{\Sigma}C$ and ${}^{12}_{\Sigma}Be$ in jj-coupling is predicted[28] to be about 3.5 if these states are purely I=1/2 and I=3/2, respectively. If $\Sigma^0 + {}^{11}C$ and $\Sigma^+ + {}^{11}B$ are approximate eigenstates of ${}^{12}_{\Sigma}C$ rather than linear combinations of good I, on the other hand, the widths become comparable. In the latter case, narrow Σ states could occur in the (K^-,π^-) reaction which were not already seen in ${}^{12}C(K^-,\pi^+)$, which selects I=3/2, $I_z = -3/2$ final states.

The case of ${}^{6}Li(K^-,\pi^+){}^{6}H$ provides the best test of the selectivity mechanism to date. The data shown in Fig. 11 display two distinct peaks, at roughly 7 and 22 MeV of excitation energy. The upper peak is seen to be narrower, with a width of 3 MeV consistent with the experimental resolution. In ref. 27, these data are given a quantitative interpretation in terms of $P_N \to P_\Sigma$ and $P_N \to S_{\Sigma^{-1}}$ transitions (lower peak) and the $S_N \to S_\Sigma$ transition (upper peak). Sine the S_N^{-1} hole strength in ${}^{6}Li$ is known to be dominated by a very narrow ($\Gamma \approx 100$ keV) ${}^{5}He$ $3/2^+$ excited state at 16.76 MeV, coupling a Σ in the 1S to this core state to form 1^+ produces a narrow state, in analogy to a similar $S_N \to S_\Lambda$ transition observed in ${}^{6}_{\Lambda}Li$ (see Fig. 5). For Σ^-, the cluster decomposition expected for this state is

$$\left[{}^{4}_{\Sigma}n(I=3/2,\ I_3=-3/2, S=0) \otimes d\right]_{1^+} . \qquad (4)$$

Since ${}^{4}_{\Sigma}n$ has the structure ${}^{4}_{\Sigma}n = (\Sigma^- p)_{S=0}(nn)_{S=0}$, the Σ^- can only convert to Λ on the proton in the deuteron cluster, and the width remains small.

In ref. 27, angluar distributions for the reaction ${}^{6}Li(K^-,\pi^+){}^{6}_{\Sigma}H$ at 720 MeV/c are calculated in the eikonal DWIA approximation. The ratio of cross sections in the two peaks is consistent with the data in Fig. 11. The lower bump in Fig. 9 reflects the presence of several Σ-hypernuclear states; the apparent width is then due to energy splittings of several MeV in addition to intrinsic Σ widths.

The s-shell targets ${}^{3}He$ and ${}^{4}He$ also offer interesting possibilities[28] for narrow Σ states, although no experiments have yet been attempted. In the reaction ${}^{4}He(K^-,\pi^-){}^{4}_{\Sigma}He$, for instance, one can populate two 0^+ states with I=1/2 or 3/2 from the $S_N \to S_\Lambda$ transition. Selectivity makes an enormous difference in the width of these states: the I=1/2 state is predicted to have twice the optical model width, while the I=3/2 member has essentially no $\Sigma \to \Lambda$ conversion width. To see this, consider the ${}^{4}He(K^-,\pi^+){}^{4}_{\Sigma}n$ reaction to the I=3/2 state. The

initial pp pair is in a $^1S_0$ state; after a coherent substitution $p \to \Sigma^-$, the resulting $\Sigma^- p$ pair remains as $^1S_0$. Since $\Sigma^- n$ cannot convert and $\Sigma^- p$ converts dominately in $^3S_1$, the width of the I=3/2 state should be small. The problem in observing such a state is that it may well lie fairly high in the Σ continuum.

The widths of Σ levels, as well as their energies and relative cross sections as seen in the $(K^-,\pi^\pm)$ reactions, are sensitive indicators of the degree of configuration and isospin mixing induced by the ΣN residual interaction. Many problems remain to be solved and exciting prospects for Σ-hypernuclei lie ahead.

IV. DOUBLY STRANGE HYPERNUCLEI AND DIBARYONS

We now discuss some of the future prospects for hypernuclear physics, namely the exploration of strangeness S= -2 systems via the $(K^-,K^{+,o})$ reactions. Since most of the cross sections we will discuss for double strangeness exchange reactions on nuclear targets are quite small (a few nb/sr to 1 μb/sr), these experiments would benefit enormously from the availability of intense kaon beams in the 1-2GeV/c range at a "kaon factory". Note that a higher momentum beam is required for (K^-,K^+) than for (K^-,π) studies of Λ and Σ hypernuclei, which would be optimized by beams in the 300-600 MeV/c range.

The simplest S= -2 systems beyond the $\Xi(1321)$ or $\Xi(1530)$ are dibaryons. Quark bag models[30] predict a variety of six quark states with different strangeness. There has been intense discussion on the existence of S=0 dibaryon resonances in nucleon-nucleon scattering[31], as well as possible S= -1 dibaryons seen in the Λp system[32]. In both cases, the proposed six-quark bag states are unstable with respect to strong decay. This gives rise to difficult questions of interpretation, since one must distinguish between a true dibaryon signal and a threshold enhancement produced as a coupled channel effect ($NN \leftrightarrow \Lambda N$ for S = 0, $\Lambda N \leftrightarrow \Sigma N$ for S= -1). The situation is potentially more favorable in the S= -2 sector, where the Bag Model predicts[33] a dibaryon (the H, with quark composition $(uuddss)_{0^+,I=0}$) which is stable against strong decay. The H plays a special role in multiquark (n > 3) spectroscopy, since it is the only such object which is predicted to decay weakly. In addition, it cannot be confused with a deuteron-like non-relativistic bound state, since it is supposed to be strongly bound (80 MeV or more) with respect to the $\Lambda\Lambda$ threshold. Here, we provide some estimates of the cross section for the reaction $^3He(K^-,K^+)nH$, which indicate that this process offers a most promising tool for H production.

The $(K^-,K^{+,0})$ reactions on nuclear targets provide a window on the spectroscopy of Ξ and $\Lambda\Lambda$ hypernuclear states. Such studies represent one logical next step in the evolution of hypernuclear physics (another important step would be the high resolution study of S= -1 hypernuclei). The new spectroscopy of Ξ and $\Lambda\Lambda$ hypernuclei is rich, although only a restricted portion of these states (high spin states with no spin slip) are excited with measurable cross sections in the high momentum transfer (K^-,K) reaction. One goal of these studies would be to extract information on the single particle properties of a Ξ in the nucleus, i.e. the real and imaginary well depths and the one-body spin-orbit potential. Narrow Ξ states are likely to exist; their widths depend delicately on the hypernuclear wave functions as well as the (essentially unknown) rate for the $\Xi N \to \Lambda\Lambda$ conversion process. One might also ultimately hope to learn something about the $\Lambda\Lambda$ and ΞN residual interactions, which would be useful in extending our knowledge of the SU(3) structure of baryon-baryon forces.

Let us first discuss the production of Ξ or $\Lambda\Lambda$ hypernuclear states. The formation of Ξ hypernuclei in the one step process $K^-p \to K^+\Xi^-$ has been discussed by Dover and Gal[34], to which we refer the reader for details. The cross sections for this process are as large as 1 μb/sr for selected high spin Ξ states. The width of the states, as governed by the process $\Xi^-p \to \Lambda\Lambda$, is estimated[34] to be small in some cases.

Double Λ hypernuclei may be formed in the (K^-,K^+) or (K^-,K^0) reactions via two-step processes $\bar{K}N \to \pi\Lambda$ followed by $\pi N \to K\Lambda$ or $\bar{K}N \to K\Xi$ plus $\Xi N \to \Lambda\Lambda$. These two mechanisms, shown in Fig. 13, are expected to be well separated kinematically. The $\bar{K}N \to K\Xi$ process peaks around 1.8 GeV/c, while $\pi N \to K\Lambda$ is maximal at a much lower pion momentum about 1.02 GeV/c, corresponding to a kaon momentum of 1.1 GeV/c. We concentrate on this latter process here, providing estimates of (K^-,K^+) cross sections for discrete $\Lambda\Lambda$ hypernuclear states. Earlier estimates focussed on sum rules[35], which indicated that most of the (K^-,K^+) strength (a few μb/sr) went into the quasielastic part of the $\Lambda\Lambda$ spectrum (because of the sizable momentum transfer). Here we concentrate on the very small cross sections (a few nb/sr) to discrete $\Lambda\Lambda$ states.

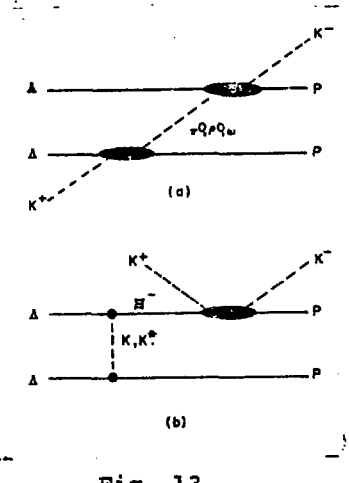

Fig. 13. Mechanism for $\Lambda\Lambda$ hypernuclear formation in the (K^-,K^+) reaction.

To estimate the $\Lambda\Lambda$ cross sections via the two-step process $K^- p \to \pi^0 \Lambda$, $\pi^0 p \to K^+ \Lambda$, we have adapted[36] the coupled channel code[37] CHUCK to the present situation. Back coupling is neglected, so our results are equivalent to second order DWBA. Full distortions of the K^-, π^0, and K^+ waves are included, using optical potentials of Woods-Saxon shape which are adjusted to reproduce the available scattering data[15] for K's and π's on ^{12}C at 800 MeV/c. Bound state wave functions for protons and Λ's in a Woods-Saxon potential are used to generate transition form factors; the parameters of the well are adjusted to reproduce the appropriate separation energies.

As a typical example, the reaction $^{16}O(K^-,K^+)^{16}_{\Lambda\Lambda}C^*$ has been investigated[36] at 1.1 GeV/c. As for the Ξ hypernuclei, the highest spin states of the $\Lambda\Lambda$ hypernucleus are preferentially populated in the (K^-,K^+) reaction, since the momentum transfer is of order 400 MeV/c, even at 0°. Some of the states expected in $^{16}_{\Lambda\Lambda}C$ are shown in Fig. 14. We indicate only natural parity states obtained by coupled $(s_\Lambda s_\Lambda)_{L=S=0}$, $(s_\Lambda p_\Lambda)_{L=1,S=0}$ or $(p_\Lambda p_\Lambda)_{L=2,S=0}$ $\Lambda\Lambda$ pairs to the 0^+ ground state of the ^{14}C core and the 2^+ core excited state at about 7-8 MeV. The latter state in ^{14}C is particularly relevant in a weak coupling picture of $^{16}_{\Lambda\Lambda}C$, since in the

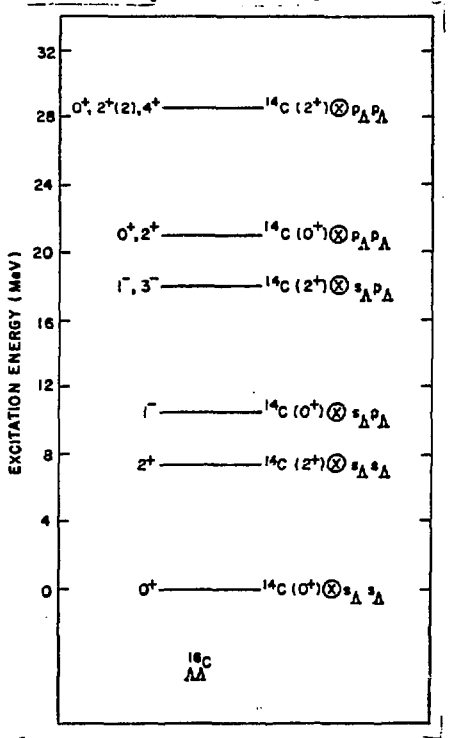

Fig. 14,
Natural parity levels in $^{16}_{\Lambda\Lambda}C$.

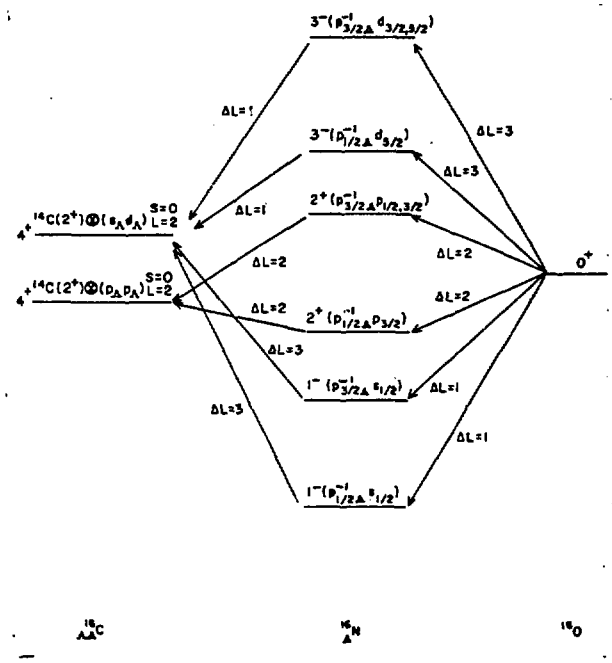

Fig. 15.
Routes from the 0^+ target ^{16}O to the 4^+ states in $^{16}_{\Lambda\Lambda}C$.

shell model it is a relatively pure two-hole state, i.e. $^{16}O(g.s.) \approx (p_{3/2}^{-1}p_{1/2}^{-1})_{L=2,S=0}$. The other low lying core states in ^{14}C are dominately of 3 hole-1 particle or 4 hole-2 particle character with respect to ^{16}O, and do not enter in the weak coupling limit considered here. The highest spin bound state of $^{16}_{\Lambda\Lambda}C$ which would be populated in the (K^-,K^+) reaction is the 4^+ configuration of structure $^{14}C(2^+) \otimes (p_\Lambda p_\Lambda)_{L=2,S=0}$. Note that the spin-flip amplitudes for both $\bar{K}N \to \pi\Lambda$ and $\pi N \to K\Lambda$ are rather unimportant, so we consider only natural parity states in the intermediate nucleus $^{16}_{\Lambda}N$ and S = 0 $\Lambda\Lambda$ pairs in $^{16}_{\Lambda\Lambda}C$. The possible routes to 4^+ final states for the two-step (K^-,K^+) process which we consider are shown in Fig. 15. Each transition is labelled by the orbital angular momentum transfer ΔL, which also equals ΔJ (since $\Delta S=0$). The transition to the $p_\Lambda p_\Lambda$ final state is seen to proceed in two successive $\Delta L=2$ transitions via $(p_\Lambda p^{-1})_{2^+}$ states in $^{16}_{\Lambda}N$, for example: In Fig. 16, we show the (K^-,K^+) cross sections[36] to selected states in $^{16}_{\Lambda\Lambda}C$. Note that one can populate unnatural parity states in $^{16}_{\Lambda\Lambda}C$ at $\theta \neq 0^o$, even in the absence of spin flip in either of the two-body reactions, but the cross sections are negligible. The (K^-,K^+) cross section to the $^{16}_{\Lambda\Lambda}C$ ground state is also seen to be small (low spin). In Fig. 17, we display the (K^-,K^+) excitation function at 0^o. We include the $^{16}_{\Lambda\Lambda}C$ states of Fig. 14. The largest cross section to a $\Lambda\Lambda$ bound configuration goes

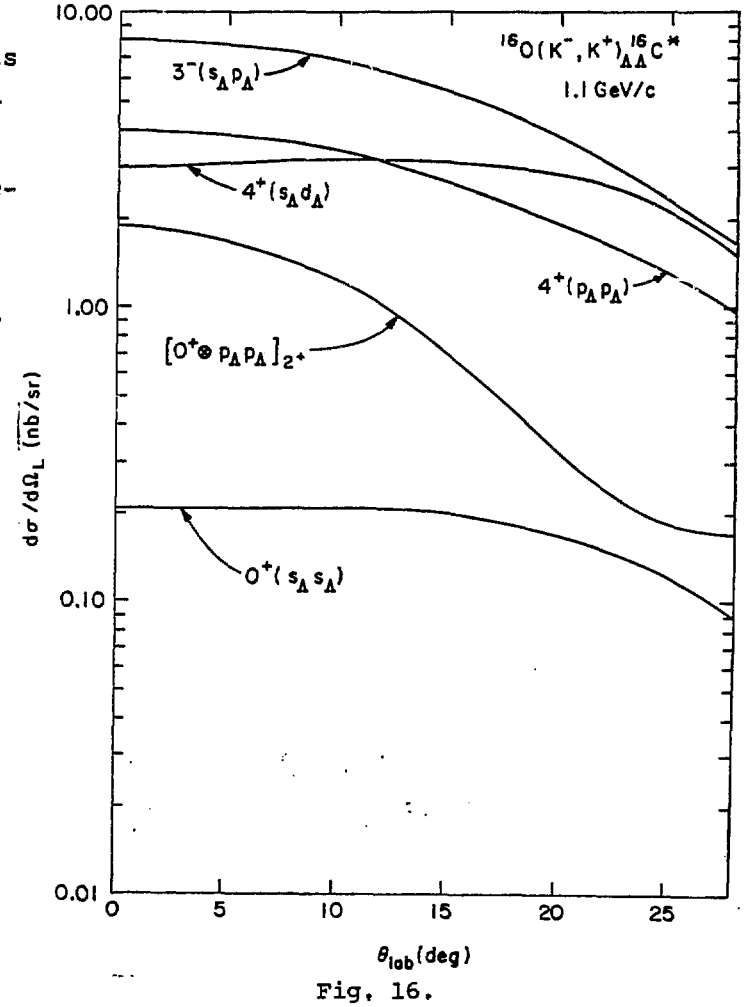

Fig. 16.

(K^-,K^+) differential cross sections to states in $^{16}_{\Lambda\Lambda}C$.

to the 3^- state. The strength associated with the continuum $s_\Lambda d_\Lambda$ configuration has been spread over about 15 MeV, roughly the escape width of the d_Λ. The other states are provided with a width of 2 MeV, to account for experimental resolution.

We have made some attempts[36] to determine an optimum target for (K^-,K^+) reactions, in order to provide the best matching of ΔJ and q. In addition to ^{16}O, another good example seems to be ^{40}Ca. In this mass region, the d_Λ single particle state is just bound (by $\sim$ 1 MeV), so one can have successive $d \to d_\Lambda$ transitions to particle stable states in $^{40}_{\Lambda\Lambda}Ar$. In the shell model, the ^{38}Ar core has a 4^+ excited state which has a sizable component $^{40}Ca \otimes (d^{-1}d^{-1})_{L=4,S=0}$. In the weak coupling picture, we obtain a high spin 8^+ state by coupling a $(d_\Lambda d_\Lambda)_{L=4,S=0}$ pair to this 4^+ core state. The (K^-,K^+) cross section to this state is of the order of a few nb/sr, as for an ^{16}O target.

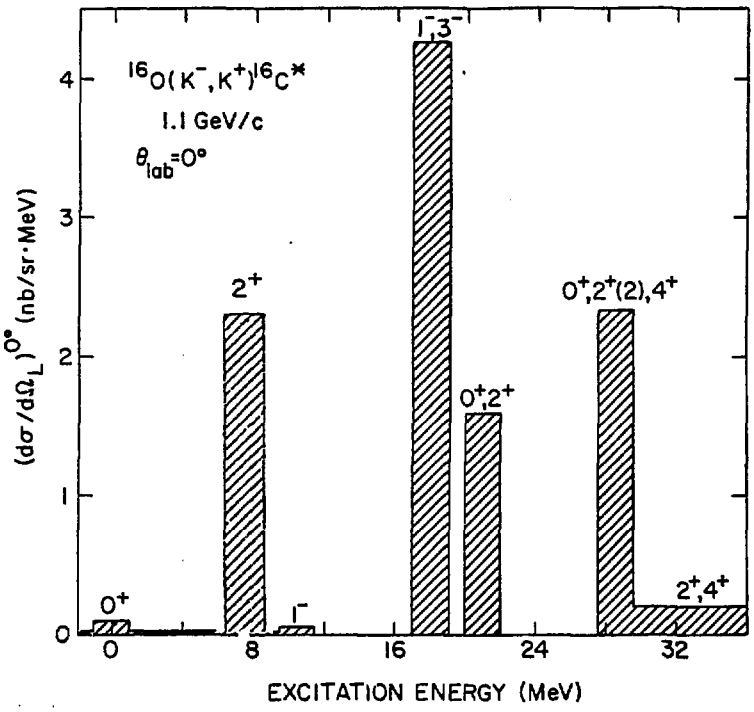

Fig. 17,
Excitation function at 0^o for $^{16}O(K^-,K^+)^{16}_{\Lambda\Lambda}C$ at 1.1 GeV/c.

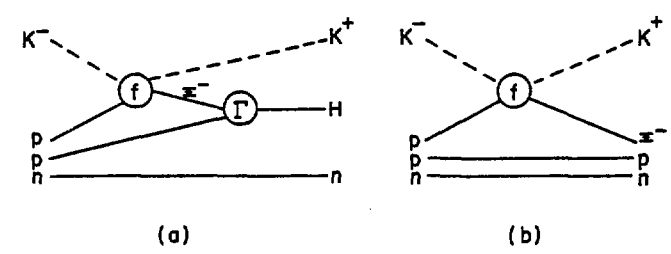

Fig. 18,
Reaction mechanism for H production on a ^3He target.

We now turn to the question of the doubly strange H dibaryon. Quark "molecules" with more complicated structures than QQQ or $Q\bar{Q}$ have often been discussed theoretically and searched for experimentally, for instance $Q^2\bar{Q}^2$

"baryonium" states, $Q^4\bar{Q}$ Z^* resonances, and Q^6 dibaryon states. The Q^6 states come with various values of strangeness. For S=0 and S= -1, many states have been predicted, and some experimental candidates exist[31,32]. The problem is that all of these Q^6 states have strong decay channels available, and so it is difficult to disentangle multiquark bag states from cross section enhancements due to coupled channel effects near thresholds. This is true for structures seen in NN scattering near the NΔ threshold and in the Λp system near the ΣN thresholds. The S= -2 sector is unique, in that it offers a candidate for a six quark state which is stable against strong decay. This particle, the H, was first proposed by Jaffe[33]. It has quantum numbers $J^\pi = 0^+$, I = 0, and a predicted mass some 80 MeV below the ΛΛ threshold, around m_H = 2150 MeV. The quark composition of the H is uuddss, with all six quarks in the lowest s-state. Such an object could be formed by a fusion of two three-quark bags, without the need for any quarks to be promoted to higher orbitals (for NN, in contrast, some quarks must be pushed up to the p-state to satisfy the Pauli principle in the six quark bag). Clearly, the fact that all quarks occupy s-states in the H contributes to its appreciable "condensation energy" with respect to two Λ's. As an amusement, one might also imagine other stable multiquark objects of this type, an example

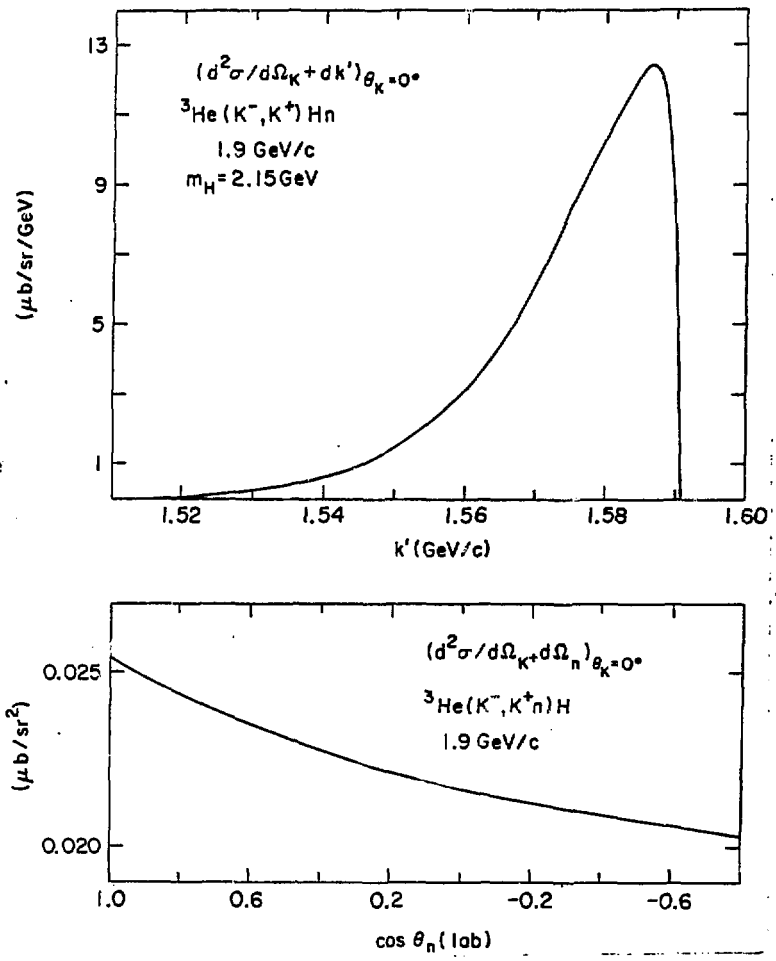

Fig. 19.
Differential cross sections for H production on ^{3}He. The upper curve shows the momentum spectrum of the K^+ at $0^{o'}$. The lower curve gives the neutron angular distribution.

being a "Noah's Ark" particle with all quark species present in pairs: $(uuddsstt\bar{b}\bar{b}cc)_{0^+,I=0}$.

One might ask whether an object with the quantum numbers of the H can be produced in ordinary potential models. Using the SU(3) model of deSwart et al[26], one can construct $\Lambda\Lambda$ and Ξ^-p potentials from various meson exchanges in the $^1S_0$,I=0 channel. Because of the absence of a one pion exchange term, the attractive potentials in this channel (or any other) are not sufficient to support any S= -2 bound state. Thus the H, if it exists, is clearly not a non-relativistic two-body bound state.

To get an idea of how to produce the H, it is useful to note its approximate wave function decomposition[38]:

$$\psi_H \approx \sqrt{4/5}\,|8_c \otimes 8_c> + \sqrt{1/10}\,|\Xi N>_{I=0} + \sqrt{1/40}\,|\Lambda\Lambda> + \sqrt{3/40}\,|\Sigma\Sigma>_{I=0}. \qquad (5)$$

When grouped into two three-quark states, we see that the H prefers to dissociate into color octets. The most favorable observable channel is ΞN, which enjoys 10% of the probability. An attempt to find the H in the reaction $pp \to K^+K^+H$ was made[39] at Brookhaven, but the cross section limits are not very restrictive. The simplest mechanism for this reaction involves two $p \to K^+\Lambda$ dissociations, followed by $\Lambda\Lambda \to H$ recombination. However, the Λ's are in general far off-shell and have a large relative momentum, which is unfavorable for H formation; quasielastic $\Lambda\Lambda$ production is much more likely. A more natural way to produce the H is via the (K^-,K^+) or (K^-,K^0) reactions. Here one brings in one unit of strangeness, which obviates the need for using double associated production. The mechanism for the prototype reaction $^3He(K^-,K^+)Hn$ is shown on the left in Fig. 18. The process $K^-p \to K^+\Xi^-$ is followed by Ξ^-p fusion to form the H. The quasielastic background is generated by the process on the right. Note that ^3He is the simplest target which supplies a diproton; since the pp pair is automatically in a $^1S_0$ state and the $K^-(pp) \to K^+(\Xi^-p)$ reaction has no spin-flip at 0°, the Ξ^-p pair is also a $^1S_0$ and hence in the correct spin state to form an H. In reactions $K^-d \to K^+(\Xi^-n)_{I=1}$ or $K^-d \to K^0(\Xi^-p)_{S=1}$ at 0°, on the other hand, the Ξ^-N pair is prepared with the wrong isospin or spin to become an H.

There are other advantages of the process of Fig. 18 for H production. The elementary 0° lab cross section for $K^-p \to K^+\Xi^-$ is not small ($\approx$40μb/sr at 1.8 GeV/c).

Also, the Ξ^- recoils with a lab momentum around 400 MeV/c; thus the Ξ^-p relative momentum p_R can be fairly small for protons near the Fermi surface. In calculating the cross section for H formation à la Fig. 18, we[40] have used an expression for the $\Xi^-p \to H$ vertex Γ motivated by the harmonic oscillator quark model: $\Gamma = \Gamma_o \exp(-p_R^2 R_H^2/12)$, where R_H is the bag radius of the H, and Γ_o contains the color-spin-flavor recoupling coefficient and geometrical factors involving the bag radii. This expression for Γ emphasizes the importance of having low p_R to obtain a sizable $\Xi^-p \to H$ fusion probability. For the ^{3}He wave function, we have used a simple product of harmonic oscillator functions in the relative momenta. Plane waves are used for the K^-, K^+, n and H. Preliminary results for the H production cross sections on a ^{3}He target are shown in Figs. 19 and 20. In a missing mass experiment, in which both the K^+ and neutron are detected, the H would show up as a well defined peak which, if m_H is well below the $\Lambda\Lambda$ threshold, is nicely separated from the broad quasielastic background. One may also consider heavier targets, which provide more di-proton pairs, but are more subject to distortion effects. The effective number of pp pairs is expected to grow much less rapidly than $Z(Z-1)$, due to absorption (particularly of the K^-), in analogy to the very slow N dependence of the effective neutron number in (K^-,π^-) reactions[9]. The ^{3}He(K^-,K^+n)H reaction is the cleanest case, if both K^+ and neutron are detected in coincidence. This experiment is well worth doing: it tests a crucial prediction of the MIT bag model, i.e., the existence of the stable H, and may provide the first definitive example of an n quark state with $n \geq 4$.

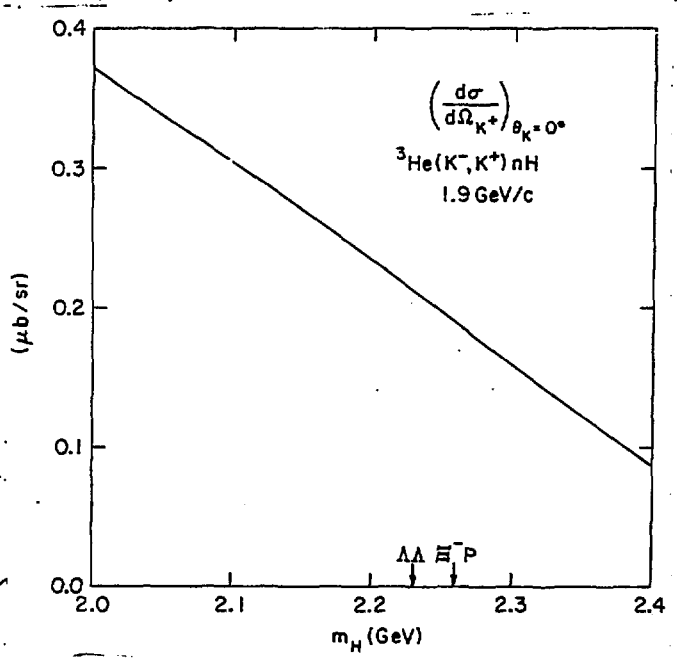

Fig. 20.

Differential cross section for H production (only K^+ detected) as a function of the mass of the H.

In summary, there are numerous new areas of hypernuclear physics which would be opened up if a "kaon factory" were to be built. Here, I have indicated but a few.

A much more complete discussion of the motivations for pursuing kaon physics will appear[5] in Physics Reports.

ACKNOWLEDGMENTS

I would like to thank my collaborators Ad Aerts, Tony Baltz, Avraham Gal, Sid Kahana, and John Millener for numerous discussions and comments. Much of the material presented here in preliminary form is taken from several collaborative efforts of the Brookhaven theory group, now in preparation for publication. This research was supported by the U. S. Department of Energy under Contract No. DE-AC02-76CH00016.

REFERENCES

1. A. Gal, in Advances in Nuclear Physics, Eds. M. Baranger and E. Vogt, Vol. 8 (Plenum Press, New York, 1975), p. 1.
2. B. Povh, Ann. Rev. Nucl. Part. Sci., Eds. J. D. Jackson, H. E. Gove, and R. F. Schwitters, Vol. 28 (Annual Reviews, Inc., Palo Alto, 1978), p. 1.
3. R. Dalitz, Proc. Int. Conf. on Nuclear Physics, Berkeley, 1980, Eds. R. M. Diamond and J. O. Rasmussen (North Holland, Amsterdam, 1981), p. 101.
4. C. B. Dover, Proc. Int. Conf. on High Energy Physics and Nucl. Structure, Versailles, July, 1981; Nucl. Phys. A374, 359c (1982).
5. C. B. Dover and G. E. Walker, "The Interaction of Kaons with Nucleons and Nuclei", to appear in Physics Reports.
6. Proc. Int. Conf. on Kaon and Hypernuclear Physics, Heidelberg, June, 1982, to be published.
7. C. B. Dover, L. Ludeking and G. E. Walker, Phys. Rev. C22, 2073 (1980).
8. G. C. Bonazzola et al, Phys. Rev. Lett. 34, 683 (1975); W. Brückner et al, Phys. Lett. 62B, 481 (1976) and Phys. Lett. 79B, 157 (1978).
9. R. Bertini et al, Nucl. Phys. A368, 365 (1981).
10. Fig. 4 was supplied by P. Barnes.
11. R. Chrien et al, Phys. Lett. 89B, 31 (1979).
12. M. May et al, Phys. Rev. Lett. 47, 1106 (1981).
13. E. H. Auerbach et al, Phys. Rev. Lett. 47, 1110 (1981).
14. E. H. Auerbach et al, submitted to Annals of Physics.

15. D. Marlow et al, Phys. Rev. C25, 2619 (1982).
16. A. Bouyssy, Phys. Lett. 91B, 15 (1980).
17. M. May, in ref. 6.
18. R. H. Dalitz and A. Gal, Ann. of Phys. 116, 167 (1978).
19. S. Cohen and D. Kurath, Nucl. Phys. 73, 1 (1965); Nucl. Phys. A101, 1 (1967).
20. R. Bertini et al, Phys. Lett. 90B, 375 (1980).
21. H. Piekarz et al, Phys. Lett. 110B, 428 (1982).
22. W. Brückner, in ref. 6.
23. C. Batty, Phys. Lett. 87B, 324 (1979).
24. R. Brockmann and W. Weise, Nucl. Phys. A355, 365 (1981); C. B. Dover and A. Gal, BNL report 30124; A. Bouyssy, Nucl. Phys. A381, 445 (1982).
25. H. J. Pirner, Phys. Lett. 85B, 190 (1979).
26. M. M. Nagels, T. A. Rijken and J. J. deSwart, Phys. Rev. D12, 744 (1975); D15, 2547 (1977); D20, 1633 (1979).
27. C. B. Dover and A. Gal, Phys. Lett. 110B, 433 (1982).
28. A. Gal and C. B. Dover, Phys. Rev. Lett. 44, 379 and 962 (1980).
29. L. S. Kisslinger, Phys. Rev. Lett. 44, 968 (1980); L. N. Bogdanova and V. E. Markushin, JETP Lett. 32, 330 (1980); W. Stepien-Rudzka and S. Wycech, Nucl. Phys. A362, 349 (1981); J. Dabrowski and F. Rozynek, Phys. Rev. C23, 1706 (1981); J. Johnstone and A. W. Thomas, TRIUMF preprint (1981).
30. R. L. Jaffe, Phys. Rev. D15, 267 and 281 (1977); A. T. M. Aerts, Nijmegen Thesis (1979).
31. N. Hoshizaki et al, Prog. Theor. Phys. 60, 1796 (1978) and 61, 129 (1979); W. Grein and P. Kroll, Phys. Lett. 96B, 176 (1980); objections to the dibaryon interpretation have been raised by P. J. Mulders, Phys. Rev. D25, 1269 (1982) and W. M. Kloet and R. R. Silbar, Nucl. Phys. A364, 346 (1981), among others.
32. O. Braun et al, Nucl. Phys. B124, 45 (1977).
33. R. L. Jaffe, Phys. Rev. Lett. 38, 195 (1977).
34. C. B. Dover and A. Gal, submitted to Annals of Physics.
35. C. B. Dover, Nukleonika 25, 521 (1980).
36. A. J. Baltz, C. B. Dover, and D. J. Millener, manuscript in preparation.
37. P. D. Kunz, private communication.

38. R. P. Bickerstaff and B. G. Wybourne, J. Phys. G (Nucl. Phys.) 7, 275 (1981); because of a phase error, the H wave function given by these authors contains a $\Sigma^*\Sigma^*$ piece which should be lumped together with $\Sigma\Sigma$.

39. A. S. Carroll et al, Phys. Rev. Lett, 41, 777 (1978).

40. A. T. M. Aerts and C. B. Dover, manuscript in preparation.